VOJNOTEHNIČKI GLASNIK / MILITARY TECHNICAL COURIER, 2025, Vol. 73, Issue 1

Conception and application of machine learning for inductance prediction in multilayer rectangular spiral micro coils

Younes Benazzouz[a], *Djilalia* Guendouz[b]

University of Oran 2 Mohamed Ben Ahmed,Industrial Maintenance and Safety Institute (IMSI), Department of instrumentation maintenance,Laboratory of Production Engineering and Industrial Maintenance (LGPMI),Oran, People's Democratic Republic of of Algeria

[a] e-mail: benazzouzyounes14@gmail.com, **corresponding author**,
ORCID iD: https://orcid.org/0009-0004-8736-7610

[b] e-mail: lila.guen@yahoo.fr,
ORCID iD: https://orcid.org/0009-0006-7129-5960

https://doi.org/10.5937/vojtehg73-56224

FIELD: computer sciences, electronics
ARTICLE TYPE: original scientific paper

Abstract:

Introduction/purpose: This research introduces a novel approach for designing a dataset of multilayer rectangular planar coils by the integration of a complementary software tools. MATLAB works as a high-level design environment, facilitating the creation of complex geometries and FastHenry acts as a computational engine to solve Maxwell's equations and extract inductance values. Two diverse synthetic datasets are generated using advanced sampling techniques, including Latin hypercube sampling, for different configurations. These datasets are then processed and trained using machine learning algorithms to predict inductance values based on the derived geometric parameters.

Methods: Initially, MATLAB is used to generate extensive synthetic datasets, comprising 20000 rows for 2-layer coil configurations and 15000 rows for 3-layer configurations. After the generation process, the datasets are checked for the readiness for training. Six machine learning models (Gaussian Process Regressor (GPR), KNeighborsRegressor (KNN), BayesianRidge, ElasticNetCV, GammaRegressor, and Bagging Regressor) are trained and evaluated using metrics such as R^2 and RMSE. The models are further tested on unseen test data and validated using the cross-validation technique to check how much the models can generalize.

Results: The datasets were generated successfully, and the models KNeighborsRegressor, Gaussian Process Regressor (GPR), and Bagging Regressor performed the best and showed a high accuracy and low error.

Conclusion: The results show that machine learning is a practical and effective method for predicting inductance in multilayer rectangular planar coils based on the geometry.

Key words: rectangular planar micro-coil, multilayer planar coil, inductance, machine learning, synthetic dataset

Introduction

Multilayer planar coils combine superior inductance and energy efficiency properties with efficient space utilization making them ideal for compact electronic applications using a parallel architecture alignment of layers. They offer an enhanced efficiency and performance in such systems, which makes them vital for advanced applications in power transmission and high-precision energy management in modern applications (Alghrairi et al., 2022). Flexible multilayer microelectromechanical systems (MEMS) coils further improve energy efficiency and space utilization and demonstrate high integration capability in arbitrary spaces, significantly enhancing the utilization of the space magnetic field and output performance in energy harvesters; their vibration energy harvesters achieve up to a 43% increase in open-circuit voltage and compact dimensions suitable for small electronics in constrained environments (Zhang et al., 2024). Furthermore, planar on-silicon multilayer inductors have proven highly beneficial in clinical applications, particularly in electromagnetic tracking (EMT) systems. These inductors achieve a stringent requirement for precise tracking in medical environments (Sidun et al., 2023). These technologies also enable the development of wireless intracranial pressure (ICP) monitoring systems, where carefully designed spiral planar coils improve the coupling factor and detection range of miniature implanted sensors, enhancing wireless power transfer efficiency and sensor performance (Wang et al., 2018). Recent designs of wireless resistive analog passive sensors have demonstrated the feasibility of bio-signal monitoring using optimized planar spiral coil pairs which are critical for long-term body signal monitoring. By employing inductive coupling and coil design optimization with genetic algorithms, these sensors achieve high sensitivity and reliable performance (Noroozi & Morshed, 2024).

Higher inductance can be achieved by increasing the number of parallel layers. However, estimating inductance remains a challenge, as directly solving Maxwell's equations for complex shapes is impractical. To address this, a versatile analytical tool has been developed for calculating the self-inductance of planar coils with general geometries. Based on Grover’s equations, this method aims to combine speed, precision, intuitive use, and geometric flexibility (Faria et al., 2021). Additionally, inductance behavior in printed-circuit rectangular spiral coils, especially in

eddy-current testing applications, can be effectively modeled using analytical methods that simplify multi-turn geometries and account for practical PCB constraints, aiding in accurate mutual inductance prediction and design optimization without relying on coil thickness (Wu et al., 2023). In superconducting circuits, mutual coupling decreases exponentially with distance between striplines, while microstrips exhibit long-range coupling, limiting scalability for large-scale integration. In addition, analytical expressions provide inductance estimations (Tolpygo et al., 2022). Another method for calculating mutual inductance between planar spiral coils with arbitrary geometries has been proposed, using a partial inductance approach that simplifies the coils into polygonal segments, allowing accurate and generalizable analysis validated by simulations and measurements (Tavakkoli et al., 2019). All these techniques are based on equation estimation and require a precise coupling factor to determine inductance.

The integration of supervised learning has demonstrated great promise in planar coil applications. Deep learning has been applied to model complex polyphase inductive coils in wireless power transfer systems, significantly reducing computational effort while maintaining high accuracy in predicting mutual inductance, with a normalized root mean square error (NRMSE) of 3.3% and a coefficient of determination of 0.985 (Gastineau et al., 2024). In magnetic resonance imaging (MRI), deep learning has shown promise for quickly predicting RF-induced heating of conductive implants based on their geometry and position, offering a faster alternative to traditional phantom experiments (Chen et al., 2023). In single-layer planar coils, a machine learning-based method has been proposed for calculating self- and mutual inductance and multiple linear regression with polynomial features achieved near-reference precision while being orders of magnitude faster(Stillig et al., 2023). Additionally, machine learning techniques have been applied to accelerate the design of magnetic couplers for wireless power transfer systems; by training on synthetic datasets from ANSYS Maxwell, these models can efficiently predict optimal coil parameters such as inner radius and number of turns while accounting for constraints like inductance and core materials (Ding et al., 2025). After recognizing the potential of machine learning in predicting the planar coil behavior and addressing the challenges of deriving precise empirical equations, we propose a machine learning-based methodology for multilayer rectangular spiral micro-coil inductance estimation.

Diving into specific algorithms, GPR proven effective for inductance estimation under magnetic saturation, significantly reduces prediction errors from 9.6% to 4.7% by improving training datasets. Its ability to minimize computational costs while maintaining accuracy highlights its potential in inductance prediction tasks (Bayazıt et al., 2023). Furthermore, inductance modeling for planar meander structures using the Restricted Boltzmann Machine (RBM) and KNN demonstrated good performance with analytical and simulation datasets and showcase the potential of these algorithms for compact inductor designs (Ansari & Agarwal, 2024). Among those using ML, none have specifically addressed the inductance of multilayer rectangular planar coils using supervised data-driven models. The primary contributions of this work are twofold:
1- The development of a systematic methodology for designing multilayer rectangular planar coils and generating a comprehensive synthetic dataset through simulations, capturing diverse coil geometries and inductance behaviors.
2- The implementation of supervised machine learning models to predict inductance values, bypassing the computational complexity of traditional coupling factor calculations and empirical formulations. This approach offers a scalable framework for rapid and accurate inductance estimation in multilayer configurations.

Methodology flowchart

The following flowchart, shown in Figure 1, illustrates the proposed methodology for the design and inductance prediction of multilayer rectangular planar coils. This structured approach integrates all key stages, including coil conception, simulation, dataset generation, and machine learning model deployment. The process begins with geometry modeling in MATLAB, where user-defined coil specifications (e.g., turns, layer alignment, trace dimensions) are translated into precise configurations. The geometries are then discretized into nodes and segments compatible with FastHenry, an open-source field solver software used to compute inductance values through electromagnetic simulations. The resulting data combining geometric parameters and simulated inductance is preprocessed to normalize features and split into training and validation sets. Supervised machine learning models are subsequently trained to map geometric inputs to inductance outputs, with performance rigorously evaluated using metrics like RMSE and MAE. The finalized model is tested on unseen configurations to validate generalizability before deployment and that enable an accurate inductance

prediction for new designs. This structured approach bridges physical simulations with data driven modeling, which eliminates reliance on complex analytical derivations.

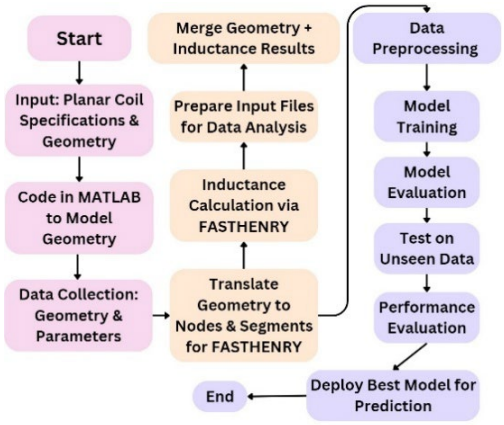

Figure 1 – Methodology flowchart for designing and predicting inductance of multilayer rectangular planar coils

Single-layer design framework for planar coils as a foundation

Before delving into the complexity of multilayer rectangular planar coils, it is essential to first understand the characteristics and behavior of a single-layer design, as it forms the basis of the multilayer coil. In the conception of planar coils for inductance estimation, a lot of estimation formulas are available such as Wheeler Expression, Modified Wheeler Expression, and Current Sheet Expression, shown in Equations 1, 2, and 3 (Wheeler, 1928) (Mohan et al., 1999), respectively. However, by analyzing these formulas, it shows that the geometry of the planar coil plays an important role in determining the inductance.

$$L_{wh} = \frac{N^2 r^2}{8r+11\Delta} \tag{1}$$

$$L_{mwh} = k_1 N_0 \frac{\mu^2 \, davg}{1+\rho k_2} \tag{2}$$

$$L = \frac{\mu_0 n^2 d_{avg} C_1}{2} \left(ln(C_2/\rho) + C_3\rho + C_4\rho^2\right) \tag{3}$$

In these equations, N represents the number of turns of the coil, and r is the radius of the planar coil. The parameter Δ is defined as half the difference between the outer and inner diameters, i.e., $\Delta = \frac{d_{out}-d_{in}}{2}$, while d_{avg} denotes the average diameter, given by $d_{avg} = \frac{d_{out}+d_{in}}{2}$. The term ρ is the fill factor, expressed as $\rho = \frac{d_{out}-d_{in}}{d_{out}+d_{in}}$. The constants k_1,k_2, C_1,C_2, C_3 and C_4 are empirical coefficients that depend on the specific geometry of the coil and μ_0 represents the permeability of free space.

By consequence, our design approach for the planar coil layer focuses on deconstructing the concept into multiple geometric variations to generate a substantial and diverse dataset for analysis, as Figure 2 shows.

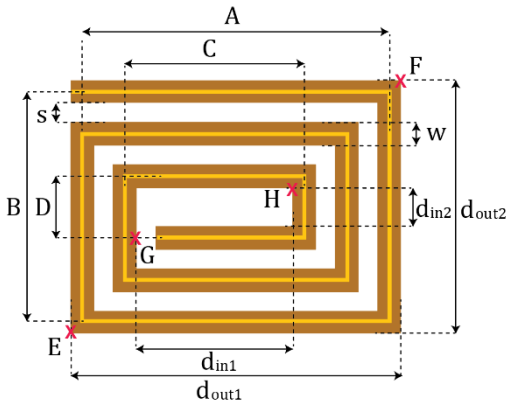

Figure 2 –2D representation of a single layer rectangular planar coil geometry with the labeled parameters

Geometric variables such as s the spacing between traces, w the trace width , n the number of turns and the inner and outer diameters d_{in1}, d_{in2} , d_{out1} and d_{out2} are commonly used and can be derived from established equations like the Wheeler's formula but these equations assume symmetrical shapes using only two diameters d_{in} and d_{out} instead of four and that reflect the symmetrical nature of the geometry. We introduced additional geometric parameters such as distances A , B , C and D in our approach of design and geometric data. Collecting these distances represents the bone diameters of the spiral shape excluding the trace width. We added hypothenuses EF and GH which are also variable distances incorporated into the design data to provide a broader range of

input parameters and to enable exploring a wider variety of geometric patterns and maximizing design versatility.,specifically $EF^2 = {d_{out1}}^2 + {d_{out2}}^2$ and $GH^2 = {d_{in1}}^2 + {d_{in2}}^2$.

Extending the single layer concept to a multilayer concept

The advantage of multilayer planar coils is their ability to increase inductance while minimizing space, making them ideal for miniaturized electronic applications. The modeling of a single layer is extended into multilayer configurations, connected in parallel through via connections that ensure seamless current flow between layers. To achieve real-world applicability, a height of 1 oz (28.35 grams) of copper material is incorporated, transforming the design into a 3D structure. Then, a FastHenry compatible input file is generated, encompassing node definitions and segment connections with material properties. This enables precise simulation of the coil's inductance and resistance, facilitating the systematic design and optimization of compact, high-inductance planar coils for advanced electronic systems. Figure 3 illustrates 3D representations of multilayer rectangular planar coils with spiral segments and via connections plotted.

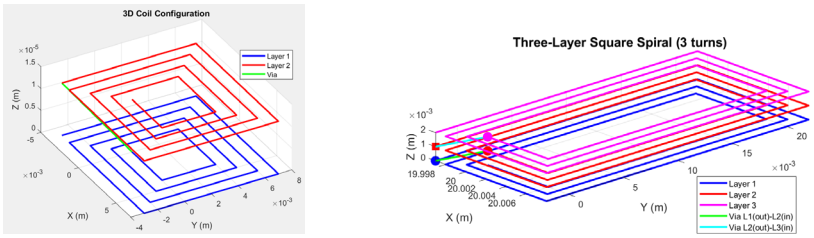

(a) 2-layer rectangular planar coil *(b) 3-layer rectangular planar coil*

Figure 3 –3D representation of a 2-layer and 3-layer rectangular planar coil with spiral segments and via connections

For multilayer planar coils, the total inductance L_T can be approximated by the sum of the self-inductances L_1, L_2 of each layer and the mutual inductance M between them (Zhao, J .2010), which is given by

$$L_T = L_1 + L_2 \pm M \tag{4}$$

$$M = 2\sqrt{L_1 L_2}\,\frac{n^2}{0.64[(0.184z^3 - 0.525z^2 + 1.038z + 1.001)(1.67n^2 - 5.84n + 65)]} \tag{5}$$

where n is the number of coil's turns, and z the distance between the layers.However, these formulas are typically valid for coils with 5 to 20 turns, and layer distances between 0.75 mm and 2 mm, are not suitable for rectangular shapes. Additionally, as the number of turns increases, the formula changes so our model will use a range of 3 to 30 turns, with wire widths varying from 40 µm to 180 µm. Unlike these analytical methods, we propose using ML to predict inductance values, which will allow us to bypass the need for these analytical formulas.

Dataset generation

After establishing the logical concept of creating multilayer planar coils, we delve into generating a dataset for training machine learning models. The dataset focuses on two configurations: two-layer and three-layer planar coils, containing 20000 rows and 15000 rows, respectively. Each row in the dataset represents a single data entry which includes multiple geometric input variables, with the output being the inductance value for each configuration.

The geometric variables include those mentioned earlier, such as the A, B, C and D segment lengths, the inner diameters and the outer diameters d_{in1}, d_{in2} , d_{out1} and d_{out2}, the spacing s, the trace width w, and the diagonals (EF, GH). In addition, the loop creation variables (i, j) are used, representing the incremental steps of the spiral design along the vertical and horizontal directions, respectively. These are defined as $i = first\ segment\ distance/\Delta x$ and $j = second\ segment\ distance/\Delta x$ where Δx is a fixed step size as shown in Figure 4.

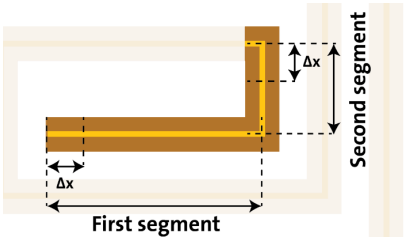

Figure 4 – Initial segments and design steps in the spiral creation

The vertical spacing between the layers, Z, represents the via distance, and that completes the foundational geometry. To enhance the dataset, feature engineering variables are introduced, such as d_{in_r} and

d_{out_r} defined as $d_{in\_r} = \sqrt{d_{in1}d_{in2}}$ and $d_{out\_r} = \sqrt{d_{out1}d_{out2}}$ respectively, These equations are adapted from the formulas used for elliptical shapes (Farooq et al. 2023) and modified for rectangular geometries by applying the area equality method, the average diameter $d_{avg} = \frac{d_{out\_r}+d_{in\_r}}{2}$, the fill ratio $\rho = \frac{d_{out\_r}-d_{in\_r}}{d_{out\_r}+d_{in\_r}}$.

These features engineered variables are commonly used in inductance estimation equations (Asadi Et all. 2023) (Wheeler, 1928). It will significantly enhance the robustness of our models and the predictive power of the dataset. This comprehensive approach ensures that the dataset captures all critical factors influencing the inductance of multilayer planar coils, making it suitable for supervised machine learning models, after defining all input parameters. A structured parameter sampling approach was implemented to generate two datasets for two and three layers planar coils. The physical and geometric parameters of the coils, along with their respective ranges, are summarized in Table 1. These ranges were chosen to cover a broad spectrum of coil designs that balance the manufacturability and performance requirements.

Table 1 – Design parameters and ranges

	Minimum Value	Maximum Value
n	3	30
i	1	15
j	1	15
w	20 μm	200 μm
s	30 μm	250 μm
z	40 μm	180 μm

To ensure a diverse and representative dataset, we combine three techniques, i.e., Latin Hypercube Sampling (LHS), parameter mapping, and physical validation and that leads us to explore a wide design space while ensuring practical manufacturability constraints were met. The main idea of LHS is dividing the range of each parameter into equally spaced intervals and it guarantees that one sample is drawn from each interval to minimize redundance in variables and clustering in the sample space. In addition, small perturbations with a value of 2% were introduced to each sampled value to simulate real word variability. Parameterization involves mapping normalized values generated through Latin Hypercube Sampling (LHS) to real-world ranges relevant to the coil design; for example, the

number of turns was mapped to [3–30], wire width to [20–200µm], and spacing to [30–250µm], while physical validation ensures that the generated coil configurations are physically feasible and adhere to manufacturability constraints with a minimum wire spacing of 30 µm to prevent electrical shorts. A layer separations [40–180µm] is compatible with standard fabrication processes.

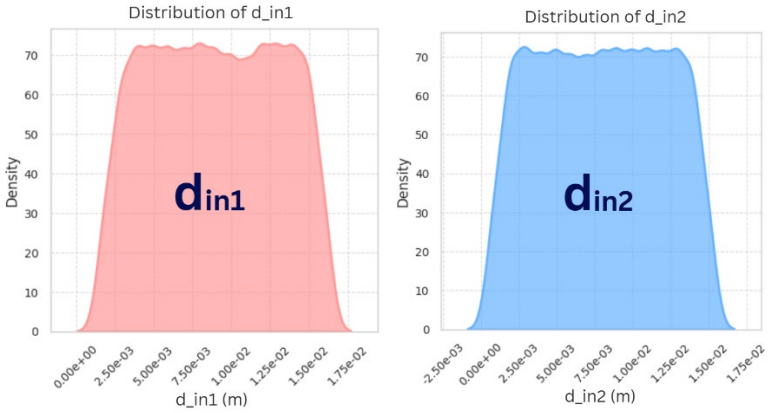

(a) Destitution of d_{in1} *(b) Destitution of d_{in2}*

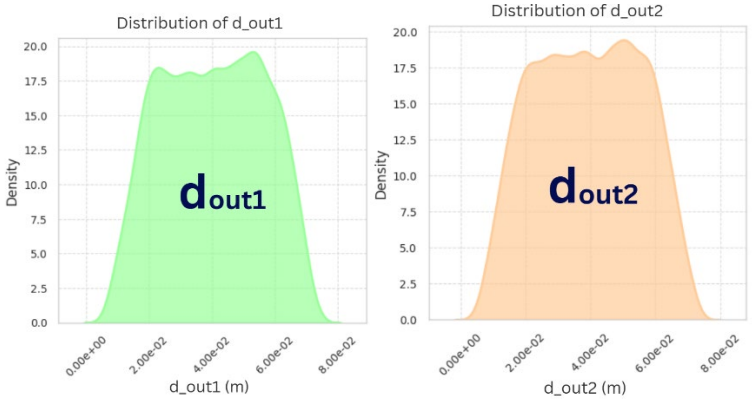

(c) Destitution of d_{out1} *(d) Destitution of d_{out2}*

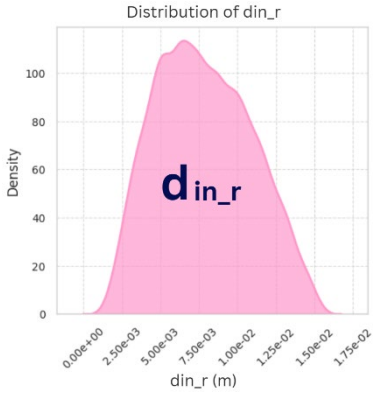

(e) Destitution of d_{in_r}

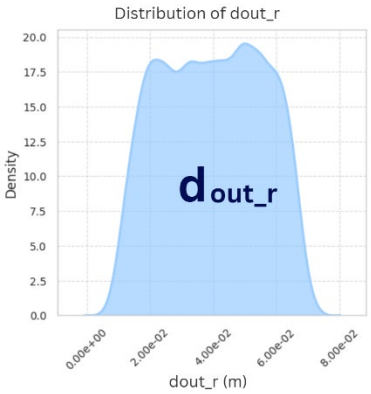

(f) Destitution of d_{in_r}

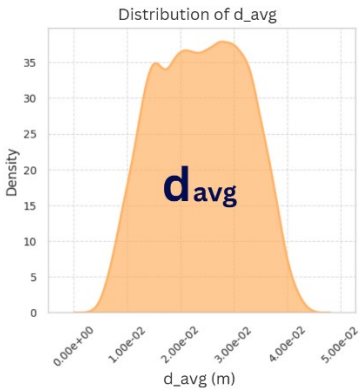

(g) Destitution of d_{avg}

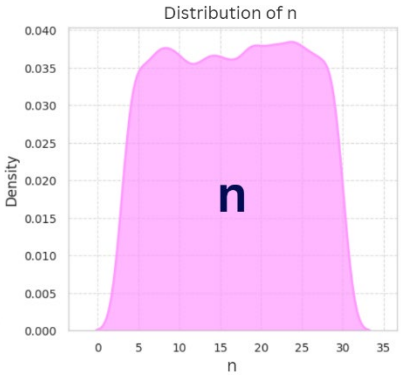

(h) Destitution of d_n

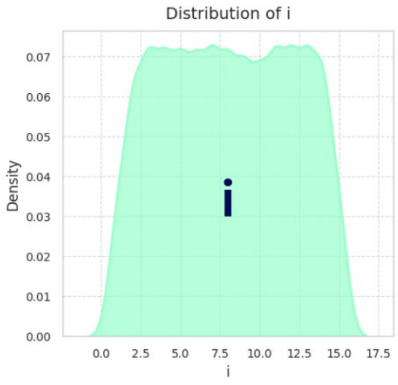

(i) Destitution of i

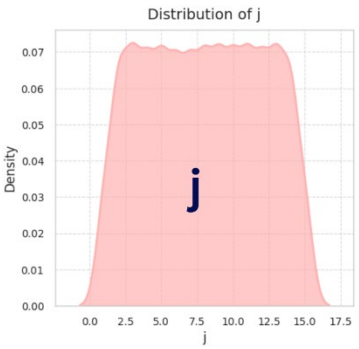

(j) Destitution of j

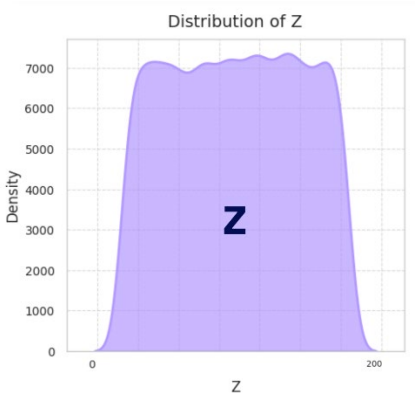

(k) Destitution of z

Figure 5 – Distribution of the geometric parameters in the 2-layer planar coil design

Figure 5 shows the density distributions of the key geometric parameters for the two-layer planar coil design and it demonstrates the effectiveness of our Latin hypercube sampling approach for multiple dimensional parameters. The inner and outer d_{in1}, d_{in2} , d_{out1} and d_{out2} diameters of the two layers show uniform distributions within their respective ranges and that indicates complete coverage of possible coil configurations. Feature engineering variables such as d_{in_r} and d_{out_r} show slightly asymmetrical distributions and the average diameter d_{avg} follows a bell-shaped distribution, suggesting a natural convergence towards optimal intermediate values. The rotation parameters n , i and j show uniform distributions in their discrete ranges, validating the efficiency of the LHS in sampling the design space. The distribution of the separation distance z guarantees adequate spacing between the layers while respecting manufacturing constraints. These distributions collectively confirm that our sampling strategy successfully explores the design space while maintaining physical feasibility, as shown by the smooth, well-defined boundaries of each parameter distribution.

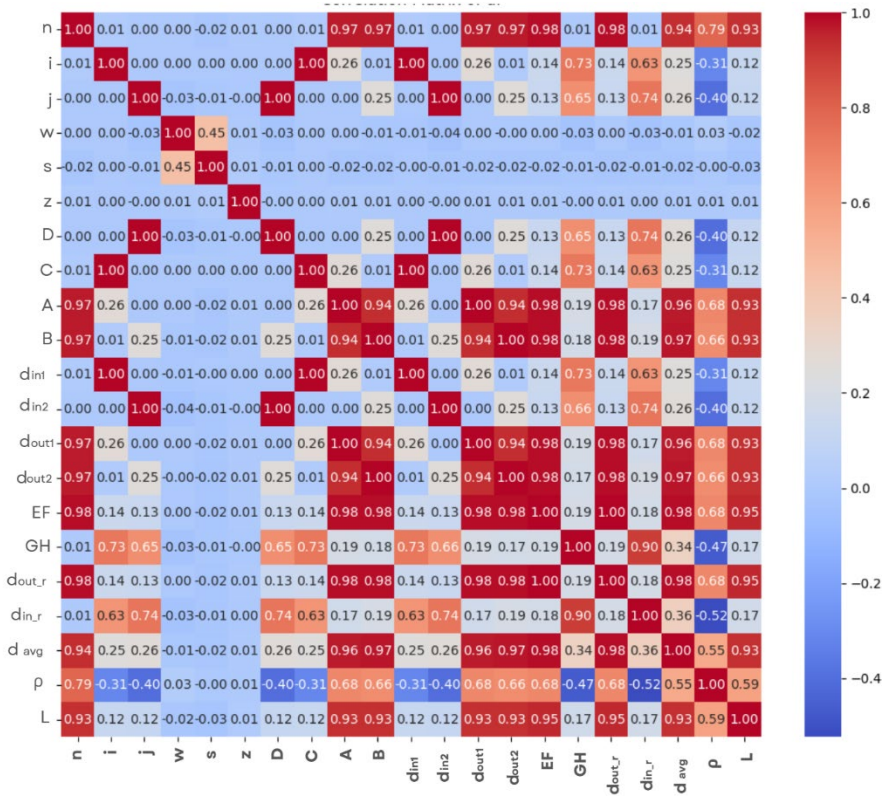

Figure 6 – Correlation matrix of the geometric variables and the inductance (L) for the two layers planar coil dataset

To gain deeper insights into the relationships among geometric variables and their influence on inductance prediction, a correlation analysis was conducted, as shown in Figure 6. The purpose of this analysis is to assess the interdependencies between the design parameters and to identify the key predictors of inductance prior to training machine learning models. The correlation matrix reveals several notable trends and positive correlations were observed between the inductance L and the parameters such as n number of turns, d_{avg} average diameter and the engineered features d_{in_r} and d_{out_r} showing a direct impact on inductance. The geometric A, B, C and D also demonstrate high correlations with L and that reflects their role in defining the overall dimensions of the coil. On the other hand, the parameters such as the (w) trace width, the spacing s, and the z vertical separation show less

correlation with L . However, even variables with weak linear correlation may contribute through non-linear interactions, especially when using models like the GPR and BaggingRegressor that can capture such complex relationships.The motivation for including both directly measured and engineered geometric variables d_{avg} , ρ d_{in_r} and d_{out_r} is based on their relevance in well-established inductance calculation equations, including those proposed in (Wheeler, 1928) (Mohan et al., 1999) and more recently in (Farooq et al. 2023). This correlation analysis serves as a foundational step to the dataset to ensure the inclusion of critical features like d_{avg} and ρ fill ratio, which give an enhancement and a predictive power of the data driven models. Furthermore, retaining a broad set of features allows machine learning models with internal feature selection mechanisms to determine their usefulness automatically.

Machine learning models selection

The data generated for inductance estimation was evaluated using various machine learning models which can be classified according to their methodologies. All models were implemented using Scikit-learn, a widely used open-source Python library that provides a consistent interface and efficient implementations for a wide range of machine learning algorithms. Unless otherwise stated, all models were used with their default parameters as defined in Scikit-learn version 1.5.2. Probabilistic models include the GaussianProcessRegressor (GPR), which assumes that the data follows a Gaussian process. As described by Rasmussen and Williams (Williams & Rasmussen, 2006), GPR predictions at a new point x^* are given by

$$f^*(x^*) = k^{*T}(K + \sigma^2 I)^{-1} y \tag{6}$$

where k^* represents the vector of covariances between x^* and the training points, K is the covariance matrix between the training points, σ^2 denotes the noise variance, I is the identity matrix and y is the vector of the training outputs.

In the category of instance-based learning, KNeighborsRegressor (KNN) was employed, a non-parametric model that predicts on the basis of nearest neighbors, thus capturing local relationships in the dataset (Altman, 1992). KNN uses the Euclidean, Manhattan and Minkowski distance metrics presented respectively:

$$d(x, X_i) = \sqrt{\sum_{i=1}^{d} \left(x_j - X_{ij}\right)^2} \quad (7)$$

$$d(x, y) = \sum_{i=1}^{n} |x_i - y_i| \quad (8)$$

$$d(x, y) = \left(\sum_{i=1}^{n} (x_i - y_i)^p\right)^{1/p} \quad (9)$$

Only one distance metric is used during model training. KNN does not use multiple distance functions simultaneously, while Euclidean measures straight-line distance in a d-dimensional space, Manhattan sums absolute differences for total travel distance, and Minkowski generalizes both, adapting to diverse data structures with the parameter p (e.g, p =2 for Euclidean, p =1 for Manhattan).

We also used linear and regularized models, such as BayesianRidge and ElasticNetCV. BayesianRidge applies Bayesian inference to linear regression, balancing bias and variance (MacKay, 1992). The model assumes

$$f(x) = \beta_0 + \beta_1 x_1^1 + \beta_2 x_2^2 + \ldots + \beta_2 x_n^n + \varepsilon \quad (10)$$

where β_i represents the coefficient and ε is the measurement error.

ElasticNetCV combines Lasso and Ridge penalties to manage multicollinearity and perform feature selection. We applied 5-fold cross-validation to automatically select the optimal values for the regularization parameters, including the overall penalty strength and the mixing ratio between the two techniques.

The BaggingRegressor model is used to combine the predictions of several instances of KNeighborsRegressor, with a total of 10 estimators in the set, each trained on different bootstrap samples of the dataset as indicated by setting (bootstrap = True).

Finally, a distribution-specific model, the GammaRegressor, has been included, designed for target variables with a Gamma distribution. The model was implemented using the default settings: alpha = 1.0 which controls regularization to balance bias and variance; link = 'log', ensuring that the predicted values remain strictly positive, suitable for Gamma-distributed targets; and solver = 'lbfgs', a quasi-Newton optimization algorithm known for efficient convergence.

To assess the performance of the machine learning models developed to estimate the inductance of multilayer planar coil designs, we employed multiple evaluation metrics. They were chosen for their ability to provide insights into the prediction capabilities of the models from different perspectives like accuracy, robustness and generalization to unseen data. By comparing these models based on these criteria, we can evaluate their suitability for inductance estimation. The metrics used for model evaluation includes the coefficient of determination R^2 and the root mean square error RMSE, which are defined by Equations (11) and (12), respectively:

$$\mathrm{R}^2 = 1 - \frac{\sum_{\mathrm{i}=1}^{\mathrm{N}} (\mathrm{y}_{\mathrm{obs,i}} - \mathrm{y}_{\mathrm{pre,i}})^2}{\sum_{\mathrm{i}=1}^{\mathrm{N}} (\mathrm{y}_{\mathrm{obs,i}} - \overline{y_{obs}})^2} \quad (11)$$

$$\mathrm{RMSE} = \sqrt{\frac{1}{\mathrm{N}} \sum_{\mathrm{i}=1}^{\mathrm{N}} (\mathrm{y}_{\mathrm{obs,i}} - \mathrm{y}_{\mathrm{pre,i}})^2} \quad (12)$$

where $\mathrm{y}_{\mathrm{obs,i}}$ is the observed inductance value, $\mathrm{y}_{\mathrm{pre,i}}$ is the corresponding predicted value, and $\overline{y_{obs}}$) is the mean of the observed inductance values. The variable n represents the total number of samples in the dataset.

Dataset splitting and models training results

All geometric variables were considered for experiment training of the selected models. The data was split into training and testing datasets with 80% used for training and 20% for testing. For the 2-layer dataset, there were 16000 samples for training and 4000 samples for testing. For the 3-layer dataset, it resulted in 12000 samples for training and 3000 samples for testing. All data was thoroughly checked for missing values, and the health of the data was verified before training to ensure that everything is perfect and all rows value are in a healthy condition.

The performance of the selected machine learning models was assessed on both training and testing datasets and through cross-validation. By this evaluation, we ensure the model's ability to generalize unseen data and avoid overfitted and underfitted models and to identify the most suitable methods for inductance prediction. Table 2 summarizes the results.

Table. 2 – Performance on train and test sets for the 2-layer planar coil

	Train set		Test set	
	R^2	RMSE	R^2	RMSE
GPR	0.999	$4.4 \cdot 10^{-9}$	0.993	$7.9 \cdot 10^{-7}$
BaggingRegressor	0.999	$3 \cdot 10^{-7}$	0.997	$4.7 \cdot 10^{-7}$
KNN	0.998	$3.2 \cdot 10^{-7}$	0.997	$5.2 \cdot 10^{-7}$
BayesianRidge	0.945	$2.3 \cdot 10^{-6}$	0.943	$2.3 \cdot 10^{-6}$
ElasticNetCV	0.922	$2.7 \cdot 10^{-6}$	0.922	$2.7 \cdot 10^{-6}$
GammaRegressor	0.760	$4.7 \cdot 10^{-6}$	0.736	$5.1 \cdot 10^{-6}$

As shown in Table 2, the Gaussian Process Regressor (GPR) demonstrated exceptional performance, achieving an R^2 of 0.999 on the training set and 0.993 on the testing set with a low RMSE, making it the top performing model. Bagging Regressor and KNN also performed well, maintaining high R^2 values on both training and testing sets and that indicates a strong predictive capability too. Linear models like Bayesian Ridge and ElasticNetCV showed moderate performance, achieving values around 0.94. The Gamma Regressor, however, displayed significantly lower R^2 square and higher RMSE values.

Table. 3 – Performance on the train and test sets for the 3-layer planar coil

	Train set		Test set	
	R^2	RMSE	R^2	RMSE
GPR	0.999	$4 \cdot 10^{-9}$	0.998	$3.2 \cdot 10^{-7}$
BaggingRegressor	0.998	$3.3 \cdot 10^{-7}$	0.998	$4 \cdot 10^{-7}$
KNN	0.998	$3.6 \cdot 10^{-7}$	0.997	$4.5 \cdot 10^{-7}$
BayesianRidge	0.943	$2.3 \cdot 10^{-6}$	0.946	$2.2 \cdot 10^{-6}$
ElasticNetCV	0.922	$2.7 \cdot 10^{-6}$	0.926	$2.6 \cdot 10^{-6}$
GammaRegressor	0.747	$4.9 \cdot 10^{-6}$	0.765	$4.7 \cdot 10^{-6}$

A similar pattern was observed for the 3-layer dataset as shown in Table 3. The GPR model again demonstrated the best performance, achieving an R of 0.999 on the training set and 0.998 on the testing set. Bagging Regressor and KNN closely followed, with minimal discrepancies between training and testing metrics. Linear models, including Bayesian Ridge and ElasticNetCV, performed consistently achieving a moderate accuracy, while the Gamma Regressor once again showed low results.

The cross-validation was applied to validate the models. This technique evaluates model performance by splitting the dataset into multiple folds and then compute the existed metrics for each fold. Table 4 summarizes the results of the cross-validation

Table. 4 – Cross-validation results using the k-fold method (k=5)

	2layers		3layers	
	R^2	RMSE	R^2	RMSE
GPR	0.998	$3.3 \cdot 10^{-7}$	0.998	$3.7 \cdot 10^{-9}$
BaggingRegressor	0.998	$3.8 \cdot 10^{-7}$	0.998	$4.1 \cdot 10^{-7}$
KNN	0.998	$4.2 \cdot 10^{-7}$	0.997	$4.5 \cdot 10^{-7}$
BayesianRidge	0.945	$2.3 \cdot 10^{-6}$	0.944	$2.2 \cdot 10^{-6}$
ElasticNetCV	0.922	$2.7 \cdot 10^{-6}$	0.923	$2.7 \cdot 10^{-6}$
GammaRegressor	0.760	$4.7 \cdot 10^{-6}$	0.754	$4.8 \cdot 10^{-6}$

The cross-validation results for both datasets confirmed the trends from experiment training and testing. In this context, the cross-validation (k=5) was applied on the training data only, in order to assess the model's robustness and consistency without involving the held-out test set. For the two-layer dataset, the GPR achieved the best performance with an R^2 of 0.998 and the lowest RMSE of $3.3 \cdot 10^{-7}$, followed by Bagging Regressor and KNN. the linear models, such as Bayesian Ridge and ElasticNetCV, showed moderate performance R around 0.94, while the Gamma Regressor struggled with the highest RMSE. Similar results were observed for the three-layer dataset, with the GPR again leading R^2 of 0.998, followed by Bagging Regressor and KNN, while the linear models performed moderately and the Gamma Regressor lagged.

Table. 6 – Monte Carlo cross-validation through 50 iterations

	2layers		3layers	
	R^2	RMSE	R^2	RMSE
GPR	0.998	$3.9 \cdot 10^{-7}$	0.998	$3.8 \cdot 10^{-9}$
BaggingRegressor	0.998	$3.8 \cdot 10^{-7}$	0.998	$4.2 \cdot 10^{-7}$
KNN	0.998	$2.24 \cdot 10^{-7}$	0.997	$4.6 \cdot 10^{-7}$
BayesianRidge	0.945	$2.27 \cdot 10^{-6}$	0.943	$2.3 \cdot 10^{-6}$
ElasticNetCV	0.922	$2.7 \cdot 10^{-6}$	0.922	$2.6 \cdot 10^{-6}$
GammaRegressor	0.760	$4.7 \cdot 10^{-6}$	0.753	$4.8 \cdot 10^{-6}$

To further validate model performance and assess robustness against data splits, Monte Carlo cross-validation through 50 iterations of randomized subsampling was applied on both 2-layer and 3-layer datasets. This method randomly splits the dataset into training (80%) and testing (20%) subsets across multiple iterations. The procedure yields distributions of performance metrics across all splits. Table 5 summarizes the performance of the models using this approach.

The Monte Carlo cross-validation results presented in Table 6 are consistent with the findings from the k-fold cross-validation presented inTable 4 and that reenforces the reliability of the models. In both the 2-layer and 3-layer datasets, the GPR consistently delivered the highest R^2 values of 0.998 and the lowest RMSE and that confirms its superior performance and robustness to data splits. Bagging Regressor and KNN also maintained strong and stable performance across all iterations. The linear models such as Bayesian Ridge and ElasticNetCV demonstrated moderate accuracy, while the Gamma Regressor exhibited the weakest results, with the highest RMSE and lowest R^2 values.

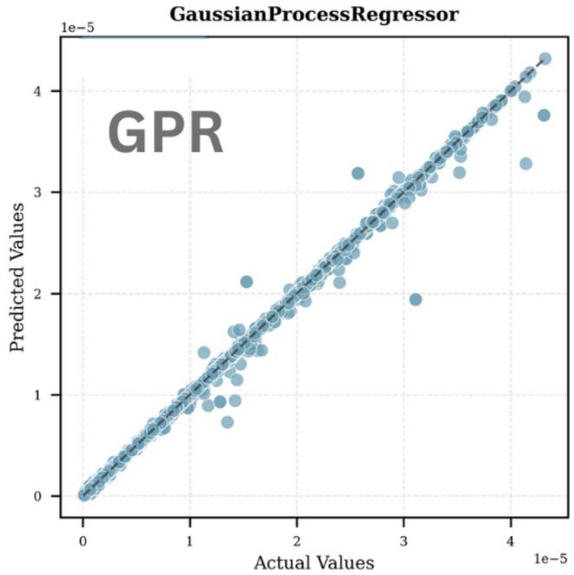

(a) Gaussian Process Regressor (GPR) – predicted vs actual values

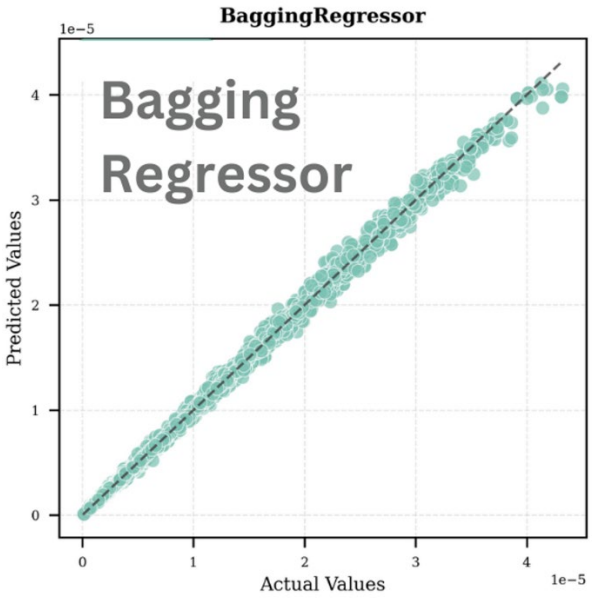

(b) *Bagging Regressor – predicted vs actual values*

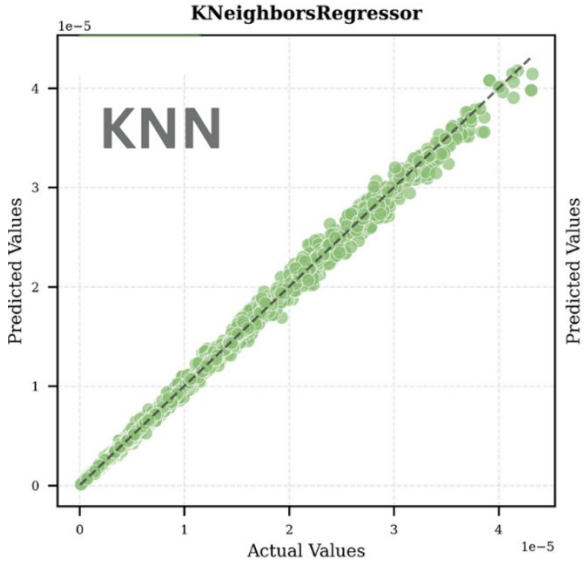

(c) K-Nearest Neighbors (KNN) – predicted vs actual values

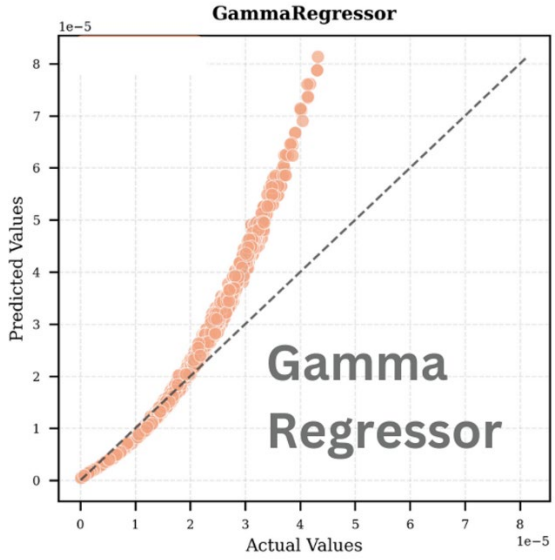

(f) Gamma Regressor – predicted vs actual values

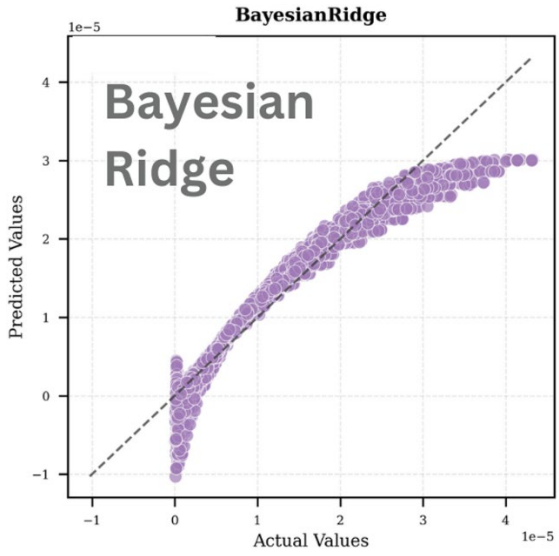

(d) Bayesian Ridge – predicted vs actual values

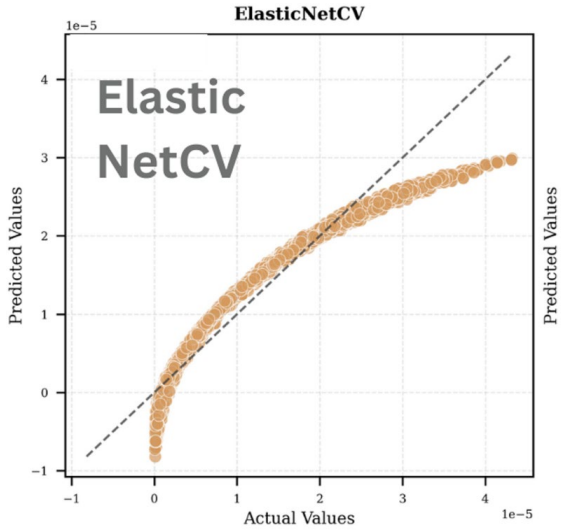

(e) ElasticNetCV – predicted vs actual values

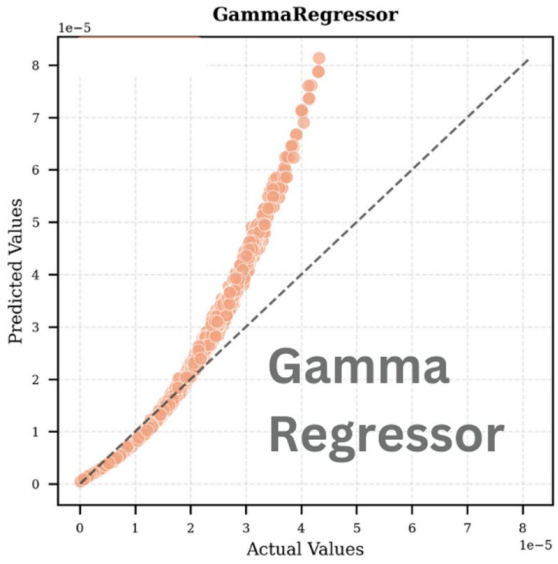

(f) Gamma Regressor – predicted vs actual values

Figure 7 – Scatter plot of predicted vs. actual values for 2-layer configurations

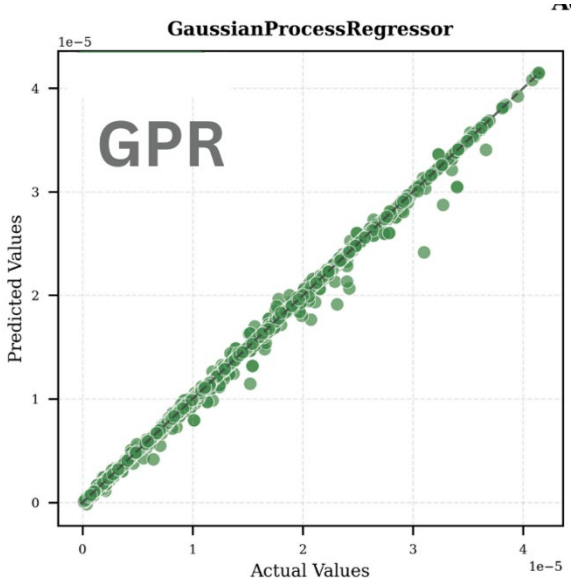

(a) Gaussian Process Regressor (GPR) – predicted vs actual values

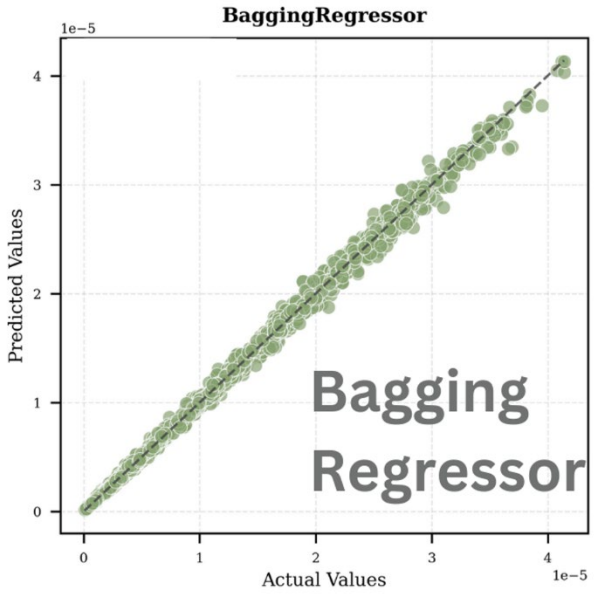

(b) Bagging Regressor – predicted vs actual values

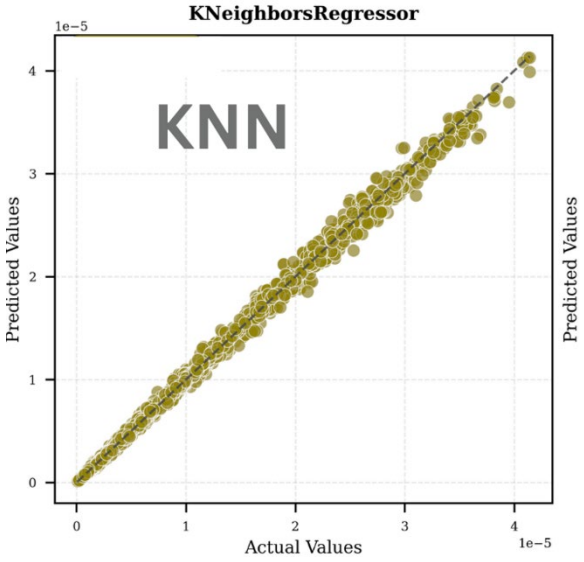

(c) K-Nearest Neighbors (KNN) – predicted vs actual values

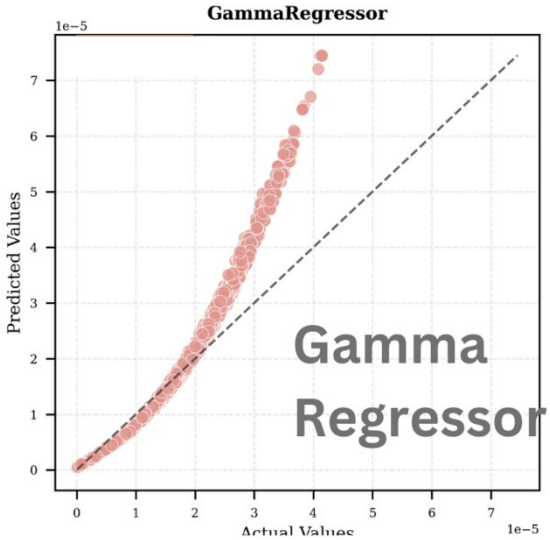

(f) Gamma Regressor – predicted vs actual values

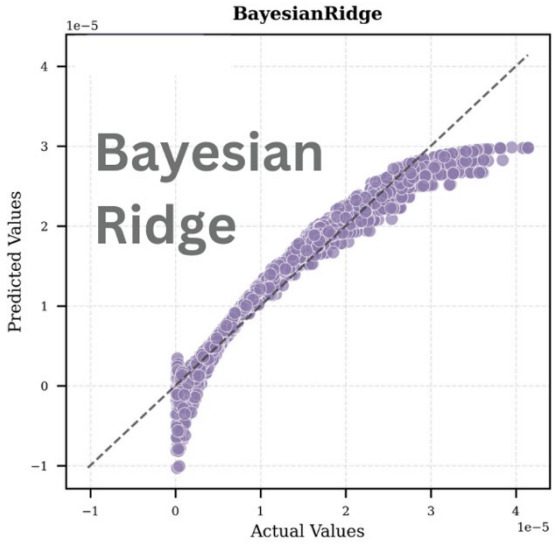

(d) Bayesian Ridge – predicted vs actual values

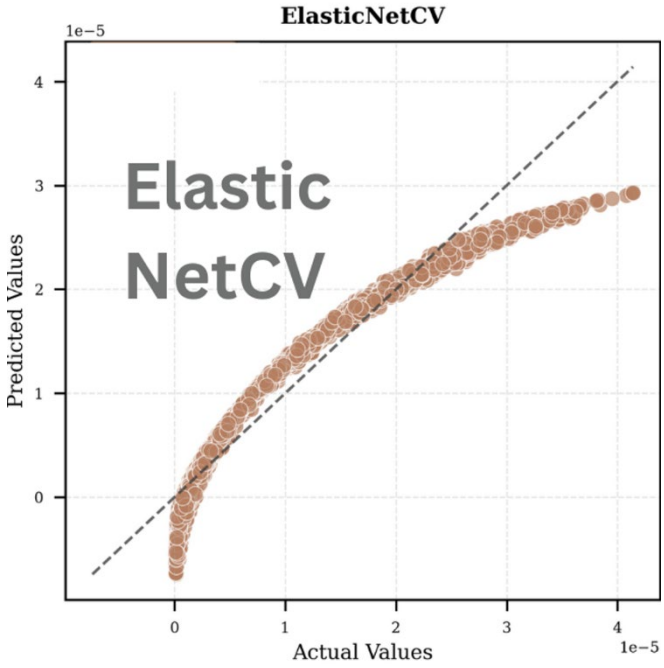

(e) ElasticNetCV – predicted vs actual values

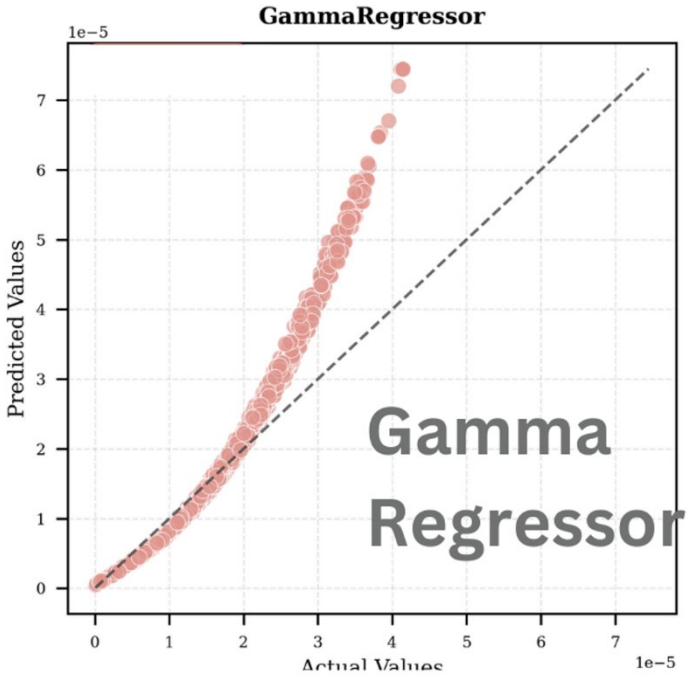

(f) Gamma Regressor – predicted vs actual values
Figure 8 – Scatter plot of predicted vs. actual values for 3-layer configurations

Figures 7 and 8 present the scatter plots of predicted versus actual values for all models across both two-layer and three-layer configurations and they provide a visual confirmation of the quantitative metrics previously discussed. The diagonal dashed line represents a perfect prediction (y=x), allowing for a direct assessment of the model performance through deviation patterns.

The GPR model exhibits remarkably tight clustering along the diagonal line in both configurations, with minimal scatter and virtually no systematic deviation, corroborating its superior R^2 value. The plot demonstrates exceptional predictive accuracy across the entire range of inductance values, with only occasional minor deviations at higher values in the three-layer configuration. The KNN and Bagging Regressor plots display similarly strong adherence to the diagonal, though with slightly more visible scatter than that of the GPR, particularly at higher inductance values. The consistency of the scatter patterns between the two-layer and three-layer configurations supports their robust generalization capabilities. In contrast, the Bayesian Ridge and ElasticNetCV models exhibit

noteworthy systematic deviations from the diagonal, particularly evident in their curvilinear patterns. These models occasionally produce negative inductance values due to their linear nature and lack of constraint mechanisms, which makes them inadequate for capturing the highly non-linear and strictly positive behavior of inductance. This behavior suggests these linear models struggle to capture the inherent non-linearities in the inductance relationships and it is manifested as a systematic underprediction at higher inductance values.

The Gamma Regressor demonstrates the most significant departure from the ideal behavior, with a distinct non-linear pattern and substantial scatter. The graph shape reveals systematic overprediction pronounced at higher inductance values and that explains the lower R^2 value. This visual evidence reinforces its inferior performance metrics and suggests fundamental limitations in capturing the underlying physical relationships.

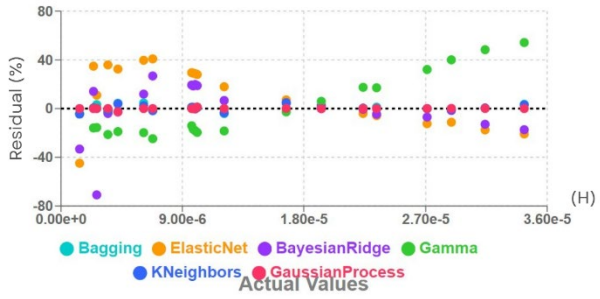

Figure 9 - Residual plot for various models of 2-layer planar coils

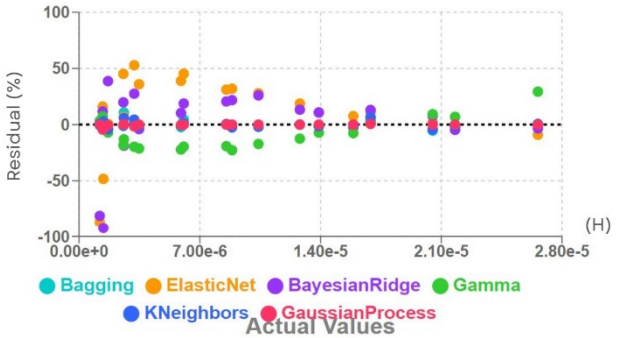

Figure 10 - Residual plot for various models of 3-layer planar coils

Testing 20 micro-planar coils with known actual inductance values, chosen randomly to ensure unbiased analysis, was visualized in Figures 9 and 10 for two-layer and three-layer configurations, respectively, and it provides evidence of model performance stability. These plots are zoomed to focus on 20 samples, allowing better visualization of variations, which is why this sample size was chosen. The plots reveal distinct error distribution patterns across different models, with the GPR, KNeighbors, and Bagging Regressor demonstrating superior prediction stability as evidenced by their tight clustering around the zero-error line, with residuals predominantly contained within a small range. This contrasts markedly with the more erratic behavior observed in the ElasticNet and Bayesian Ridge linear models, and the systematic deviations displayed by the Gamma Regressor, particularly at higher inductance values. The three-layer configuration exhibits similar patterns, though with a slight increase in residual spread, reflecting the enhanced complexity of the prediction task. Based on the comprehensive evaluation of quantitative metrics, scatter plots, and residual analyses, the GPR emerges as the optimal model for inductance prediction, followed in a close way by Bagging Regressor and KNeighbors, all demonstrating robust generalization capabilities and reliable performance on unseen data across both geometric configurations.

Conclusion

The study demonstrates a new approach based on supervised learning models to achieve high accuracy in estimating the inductance of multilayer rectangular planar coils. The methodology utilized geometric parameters to train machine learning models, with the Gaussian Process Regressor achieving superior performance, demonstrating R^2 values exceeding 0.99 for both configurations. This approach eliminates the need for complex empirical equations compared to traditional analytical methods. The proposed data-driven framework provides higher precision and adaptability to diverse rectangular multilayer coil configurations. The simulation results validated the accuracy of the machine learning models, highlighting the significant role of the parameters such as the number of turns, the average diameter, and the fill ratio in predicting inductance. As future work, the methodology can be extended to include more complex coil configurations and explore alternative shapes using other machine learning models or even using deep learning techniques to further enhance its accuracy and versatility.

References

Alghrairi, M., Sulaiman, N., Mutashar, S., Wan Hasan, W. Z., Jaafar, H., & Algriree, W. (2022). Designing and analyzing multi-coil multi-layers for wireless power transmission in stent restenosis coronary artery. *AIP Advances, 12*(12). Available at: https://doi.org/10.1063/5.0121532

Altman, N. S. (1992). An Introduction to Kernel and Nearest-Neighbor Nonparametric Regression. *The American Statistician, 46*(3), 175–185. Available at: https://doi.org/10.1080/00031305.1992.10475879

Ansari, M.A., & Agarwal, P. (2024). Inductance Modelling of Planar Meander Structure Using RBM and kNN. *SN Computational Sciences, 5*, 1169. Available at: https://doi.org/10.1007/s42979-024-03516-7

Asadi, M., Rezaei, A., & Abazari, A. M. (2023, December). Calculation of Mutual Inductance between Two Planar Coils with Custom Specifications and Positions Using a Machine Learning Approach. In *Proceedings of the International Conference on New Trends in Applied Sciences* (Vol. 1, pp. 20-30). Available at: https://doi.org/10.58190/icontas.2023.50

Bayazıt, G. H., Caarls, E. I., & Lomonova, E. A. (2023). Inductance Map Regression of Doubly Excited Electrical Machines Considering Cross-Saturation. *IEEE Transactions on Magnetics, 59*(11), 1-5. Available at: https://doi.org/10.1109/TMAG.2023.3292500

Chen, X., Zheng, C., & Golestanirad, L. (2023). Application of Machine learning to predict RF heating of cardiac leads during magnetic resonance imaging at 1.5 T and 3 T: A simulation study. *Journal of Magnetic Resonance*, *349*, 107384. Available at: https://doi.org/10.1016/j.jmr.2023.107384

Ding, W., Wang, Y., Chen, T., Lu, Z., You, Y., Wang, J., & Huang, Z. (2025). A stacking machine-learning based method for accelerating magnetic coupler design with ferrite cores in inductive power transfer applications. International Journal of Circuit Theory and Applications, 53(1), 67-80. Available at: https://doi.org/10.1002/cta.4096

Farooq, M., Amin, B., Elahi, A., Wijns, W., & Shahzad, A. (2023). Planar Elliptical Inductor Design for Wireless Implantable Medical Devices. *Bioengineering, 10*(2), 151. Available at: https://doi.org/10.3390/bioengineering10020151

Faria, A. R. S., Marques, L. S., Gaspar, J., Alves, F. S., & Cabral, J. M. N. (2021, March). High precision, geometry independent analytical method for self-inductance calculation in planar coils. In *2021 22nd IEEE International Conference on Industrial Technology (ICIT)* (Vol. 1, pp. 1234-1239). IEEE. Available at: http://doi.org/10.1109/ICIT46573.2021.9453559

Gastineau, L. A., Lewis, D. D., & Ionel, D. M. (2024, November). Combined 3D FEA and Machine Learning Design of Inductive Polyphase Coils for Wireless EV Charging. In *2024 13th International Conference on*

Renewable Energy Research and Applications (ICRERA) (pp. 1811-1816). IEEE. Available at: https://doi.org/10.1109/ICRERA62673.2024.10815533

MacKay, D. J. (1992). Bayesian interpolation. *Neural Computation, 4*(3), 415-447. Available at: https://doi.org/10.1162/neco.1992.4.3.415

Noroozi, B., & Morshed, B. I. (2021). Design and optimization of printed spiral coils for wireless passive sensors. *IET Wireless Sensor Systems*, *11*(4), 169-178. Available at: https://doi.org/10.1049/wss2.12019

Sidun, Aleksandr, SRIVASTAVA, Manish, O'DONOGHUE, Kilian, et al. Planar On-Silicon Inductor Design for Electromagnetic Tracking. *IEEE Sensors Journal, 2023*. Available at: https://doi.org/10.1109/JSEN.2023.3296471

Stillig, J., Parspour, N., Ewert, D., & Jung, T. J. (2022, July). Feasibility Study on Machine Learning-based Method for Determining Self-and Mutual Inductance. In *2022 International Seminar on Intelligent Technology and Its Applications (ISITIA)* (pp. 193-198). IEEE. Available at: https://doi.org/10.1109/ISITIA56226.2022.9855321

Tolpygo, S. K., Golden, E. B., Weir, T. J., & Bolkhovsky, V. (2022). Mutual and self-inductance in planarized multilayered superconductor integrated circuits: Microstrips, striplines, bends, meanders, ground plane perforations. *IEEE Transactions on Applied Superconductivity, 32*(5), 1-31. Available at: https://doi.org/10.1109/TASC.2022.3162758

Wang, F., Zhang, X., Shokoueinejad, M., Iskandar, B. J., Webster, J. G., & Medow, J. E. (2018). Spiral planar coil design for the intracranial pressure sensor. Medical Devices & Sensors, 1(3), e10012. Available at: https://doi.org/10.1002/mds3.10012

Wheeler, H. A. (1928). Simple inductance formulas for radio coils. *Proceedings of the Institute of Radio Engineers, 16*(10), 1398-1400. Available at: https://doi.org/10.1109/JRPROC.1928.221309

Williams, C. K., & Rasmussen, C. E. (2006). Gaussian processes for machine learning (Vol. 2, No. 3, p. 4). Cambridge, MA: MIT press.

Wu, D., Lin, S., Chen, H., & Wang, X. (2023). Mutual inductance model of double printed circuit board-based coplanar rectangular spiral coils for eddy-current testing. International Journal of Numerical Modelling: Electronic Networks, Devices and Fields, 36(1), e3038. Available at: https://doi.org/10.1002/jnm.3038

Zhang, J., Hou, X., Qian, S., Bi, X., Hu, D., Liu, J., ... & Chou, X. (2024). Flexible multilayer MEMS coils and their application in energy harvesters. *Science China Technological Sciences, 67*(4), 1282-1293. Available at: https://doi.org/10.1007/s11431-023-2474-9

Zhao, J. (2010). A new calculation for designing multilayer planar spiral inductors. *EDN (Electrical Design News, 55*(14), 37.

Концепт и примена машинског учења у предвиђању индуктивности у вишеслојним правоугаоним спиралним микрозавојницама

Јунес Беназуз, **аутор за преписку**, *Џилалија* Гендуз
Универзитет у Орану 2 Мохамед Бен Ахмед, Институт за индустријско одржавање и безбедност (IMSI), Одељење за одржавање инструмената, Лабораторија за производно инжењерство и индустријско одржавање (LGPMI), Оран, Народна Демократска Република Алжир

ОБЛАСТ: рачунарске науке, електроника
КАТЕГОРИЈА (ТИП) ЧЛАНКА: оригинални научни рад

Сажетак:

Увод/циљ: Овим истраживањем уводи се нов приступ пројектовању скупа података правоугаоних планарних завојница помоћу комплементарних софтверских алата. МАТЛАБ функционише као окружење за пројектовање високог нивоа, а FastHenry делује као рачунарски оквир за решавање Максвелових једначина и добијање вредности индуктивности. Генеришу се два различита синтетичка скупа података помоћу напредних техника узорковања за различите конфигурације, укључујући методу узорковања латинске хиперкоцке. Ови скупови података се затим обрађују и обучавају помоћу алгоритама машинског учења за предвиђање вредности индуктивности на основу добијених геометријских параметара.

Методе: За генерисање екстензивних синтетичких скупова података који садрже 20 000 редова за двослојне конфигурације завојница и 15 000 редова за трослојне конфигурације прво се користи МАТЛАБ. Након процеса генерисања, проверава се да ли су скупови података спремни за обуку. Шест модела машинског учења: Gaussian Process Regressor (GPR), KNeighborsRegressor (KNN), BayesianRidge, ElasticNetCV, GammaRegressor, као и Bagging Regressor обучено је и процењено помоћу метрика као што су R^2 и RMSE. Модели се затим испитују на непознатим подацима за испитивање и оцењују помоћу технике унакрсне валидације како би се утврдило колико могу да генерализују.

Резултати: Скупови података су успешно генерисани, а модели KNeighborsRegressor, Gaussian Process Regressor (GPR) и Bagging Regressor остварили су најбоље резултате, исказали су велику тачност и малу грешку.

Закључак: Резултати показују да је машинско учење практичан и ефикасан метод за предвиђање индуктивности у вишеслојним правоугаоним планарним завојницама на основу геометрије.

Кључне речи: правоугаона планарна микрозавојница, вишеслојна планарна завојница, индуктивност, машинско учење, синтетички скуп података

Paper received on: 22.01.2025.
Manuscript corrections submitted on:22.04.2025.
Paper accepted for publishing on: 04.06.2025.